ELSEVIER

Signal Processing 80 (2000) 1335–1346

SIGNAL PROCESSING

www.elsevier.nl/locate/sigpro

Performance bounds for cochannel interference cancellation within the current GSM standard

Hafedh Trigui*, Dirk T.M. Slock

Institut EURECOM, 2229 route des Crêtes, B.P. 193, 06904 Sophia Antipolis Cedex, France

Received 28 November 1998; received in revised form 19 March 1999

Abstract

The performance of maximum-likelihood sequence estimation (MLSE) is bounded (and often approximated well) by the matched filter bound (MFB). In this paper, we first show how the linearized GMSK modulation of GSM can be reformulated to have a real symbol constellation, leading to a two-channel aspect due to the in-phase (I) and in-quadrature (Q) components of the received signal. More channels can be added by oversampling and/or the use of multiple sensors (antennas, polarizations). Given this model, we present the MFB for MLSE single-user detection in the presence of interferers that are modeled as colored Gaussian noise. The MLSE is assumed to employ noise correlation information that in general may differ from the true one (e.g. by simplifying spatio-temporal correlations to spatial correlations only). One of the conclusions is that properly taking into account the spatio-temporal correlation of the interference leads to much improved performance (MFB) compared to purely spatial approaches. Another conclusion is that the excess bandwidth in GMSK provides some useful channel diversity. © 2000 Elsevier Science B.V. All rights reserved.

Zusammenfassung

Die Leistungsfäshigkeit des Maximum Likelihood-Folgenschätzers (MLSE) ist durch die Matched Filter-Schranke (MFB) beschränkt (und wird oft durch diese gut angenähert). In dieser Arbeit zeigen wir zunächst, wie die bei GSM verwendete linearisierte GMSK-Modulation mit einer reellen Symbolkonstellation formuliert werden kann. Aufgrund der Inphasekomponente (I) und Quadraturkomponente (Q) des empfangenen Signals führt diese Formulierung zu einer Zweikanal-Interpretation. Weitere Kanäle können durch Überabtastung und/oder durch Verwendung mehrerer Sensoren (Antennen, Polarisation) hinzugefügt werden. Unter Annahme dieses Modells präsentieren wir die MFB für MLSE-Einzelbenutzer-Detektion in Anwesenheit von Interferenz, die als farbiges Gaußsches Rauschen modelliert wird. Wir nehmen an, daß der MLSE Information über die Rausch-Korrelation verwendet, die im allgemeinen von der wahren Korrelation abweichen kann (z.B. durch Vereinfachung von Raum-Zeit-Korrelationen zu rein räumlichen Korrelationen). Eine der Schluß folgerungen ist, daß bei richtiger Berücksichtigung der Raum-Zeit-Korrelation der Interferenz die Leistungsfähigkeit (MFB) wesentlich besser ist als bei rein räumlichen Ansätzen. Eine weitere Schlußfolgerung ist, daß die Überschußbandbreite von GMSK nützliche Kanaldiversität liefert. © 2000 Elsevier Science B.V. All rights reserved.

* Corresponding author. Present address: Telecom MODUS Ltd, Cleeve Road Leatherhead, Surrey England, KT22 75A. Tel.: + 44-1372-804854; fax: + 44-1372-804804.

E-mail addresses: hafedh.trigui@t-modus.nec.co.uk (H. Trigui), slock@eurecom.fr (D.T.M. Slock).

0165-1684/00/$ - see front matter
PII: S0165-1684(00)00040-2

Résumé

La performance de la détection de séquence basée sur le critère de maximum de vraisemblance (DSMV) est bornée (et souvent bien approximée) par la borne du filtre adapté (BFA). Dans ce papier, on démontre tout d'abord que la version linéarisée de la modulation GMSK utilisée par le système GSM peut être reformulée afin d'obtenir une constellation réelle pour les symboles transmis, permettant d'avoir un aspect bivoie dû aux composantes en phase et en quadrature de phase du signal reçu. On peut obtenir plus que deux canaux en suréchantillonnant le signal reçu et/ou en utilisant plusieurs capteurs (antennes, polarisations). Pour ce modèle, on présente la BFA correspondant à la DSMV faisant la détection d'un seul utilisateur en présence des interféreurs modèlisés par un bruit Gaussien coloré. On suppose que l'information sur la corrélation du bruit exploitée par la DSMV peut être, en général, incomplète (par exemple en simplifiant les corrélations spatio-temporelles par des corrélations spatiales). Dans les conclusions, il s'avère d'une part que la prise en compte correcte des corrélations spatio-temporelles des interféreurs permet de nettement améliorer les performances (BFA) et d'autre part qu'une diversité intéressante résulte de l'exploitation de l'excès en largeur de bande de la modulation GMSK.

Keywords: Mobile communications; GSM; Matched filter bound; Interference cancellation; Spatio-temporal processing

1. Introduction

The global system for mobile (GSM) standard for second-generation cellular mobile communications is widely deployed in Europe and certain other parts of the world. The particularities of GSM that will be exploited in this paper are time division multiple access (TDMA) and cellular frequency reuse which means that the service area is covered by clusters of cells and that the available frequency band is partitioned over the cells in a cluster. The number of cells in a cluster is called the reuse factor. These characteristics also hold for the American standard IS54/136. Another beneficial characteristic is that the transmitted symbol constellation is essentially binary. This last characteristic will no longer hold for certain extensions to GSM that are currently being discussed (such as EDGE [3]). Nevertheless, most of the ideas in this paper still apply to these variations.

The popularity of GSM systems leads to the saturation of their capacity at certain strategic places. This forces operators to find a means to increase the capacity of their system. One solution is to perform interference cancellation, which allows to reduce the frequency reuse factor (for a given quality of service) and hence to increase the system capacity. The optimal way to perform interference cancellation is to jointly detect the signal of interest and the interfering signals according to the maximum-likelihood criterion, using the Viterbi algorithm (VA) [14]. However, the complexity of the VA for multi-user detection is exponential in the number of users and hence is prohibitive. Thus, suboptimal approaches are desirable. One suboptimal approach starts by recognizing the spatial dimension of the cellular multi-user problem: the interfering signals and the signal of interest typically arrive from different directions. Hence, an adaptive antenna array can be used to steer the antenna diagram towards the signal of interest while putting nulls in the directions of the interfering signals [13]. This is a form of linear multi-user detection which completely relies on the spatial dimension.

The particular approach we shall follow here consists of single-user detection in the presence of interferers considered as colored noise. Since we shall not detect the interferers, we do not exploit their discrete distribution. In fact, we wish to only exploit their second-order statistics and hence we model them as Gaussian noise. One of the main points of this paper is to show that such a suboptimal approach leads to limited performance loss compared to optimal multi-user detection if we dispose of a multichannel formulation with more channels than users (in which case zero-forcing multiple-acces interference (MAI) and intersymbol interference (ISI) cancellation is generically possible [9]). Multichannels can arise in various ways:

(1) By receiving through multiple sensors (antennas, polarizations, etc.), multiple physical channels appear.
(2) By oversampling the received signal w.r.t. the symbol rate, the polyphase components (at the symbol rate) of channel and received signal can be considered as multiple fictitious channels. E.g., for the typical oversampling factor of two, even and odd subsamples yield two fictitious channels.
(3) If the transmitted symbols are real (PAM, BPSK,...), then after modulation and demodulation, the I and Q components of the channel and received signal can be considered as two fictitious channels in a system formulation in which input, noise and output are real quantities. We shall show that after linearization and a certain demodulation, the GMSK modulation of GSM can be made to correspond to a BPSK modulation.

So for GSM, the total number of channels is typically four (two times two) times the number of receiver sensors.

With the interferers modeled as Gaussian colored noise, optimal detection becomes single-user MLSE in the presence of colored noise. The noise correlations induce a certain weighted metric to be used in the VA. In [12], we have shown that, especially when the number of channels exceeds the number of users, such MLSE performs not only equalization but also interference cancellation. Using the interference-canceling matched filter (ICMF) introduced in [12], the interference cancellation operation can be separated in a first receiver stage that concentrates the multichannel information into a single channel, on which equalization can then be performed.

As implied by the discussion above, the delay spread due to multipath propagation generally leads to ISI in GSM and hence the channel has a temporal dimension. In the multichannel model, if we call the channel index dimension the spatial dimension, then the overall multichannel is spatio-temporal. Note that for GSM, the number of channels can be up to eight times the number of antennas (if polarization diversity antennas are used). This multichannel aspect allows for a significant increase in interference cancellation capability compared to a pure antenna based approach. Furthermore, a full spatio-temporal treatment allows to properly incorporate the temporal aspect also so that zero forcing is generally possible whenever the number of channels exceeds the number of users (hence one antenna is in principle sufficient if only the interferers on the first tier are taken into account). In the purely spatial antenna processing approach though, zero forcing can only be possible if the number of antennas exceeds the total number of temporally resolvable paths (signature vectors [15]) of all users.

The rest of the paper is organized as follows. In the next section we show how GMSK can be interpreted as BPSK modulation after linearization and a certain demodulation. In Section 3, the multichannel system model is formulated. Matched filter bounds (MFBs) are derived and presented in Section 4 for single-user MLSE in colored noise. Expressions are given for both burst-mode (as in GSM) and continuous transmission. The general case of a possible mismatch between the actual and assumed noise correlations is considered. The particular case of the colored noise consisting of d interfering signals of the same form as the signal of interest plus white noise is analyzed in Section 5. Specifically, the loss in MFB compared to optimal multi-user detection is evaluated. In Section 6, a typical purely spatial processing approach is considered and its performance analyzed. In Section 7, we present the average performance of various spatio-temporal and spatial approaches for typical GSM channel models. Finally, we formulate some conclusions in the last section.

2. Linearization of a GMSK signal

We analyse first GMSK signals. Let $x(t) = e^{j\varphi(t)}$ be a baseband GMSK signal, where

$$\varphi(t) = \frac{\pi}{2}\sum_k a_k \int_{-\infty}^{t} \mathrm{rect}\left(\frac{u-kT}{T}\right) h(u)\,\mathrm{d}u$$

$$= \sum_k a_k \phi(t-kT) \qquad (1)$$

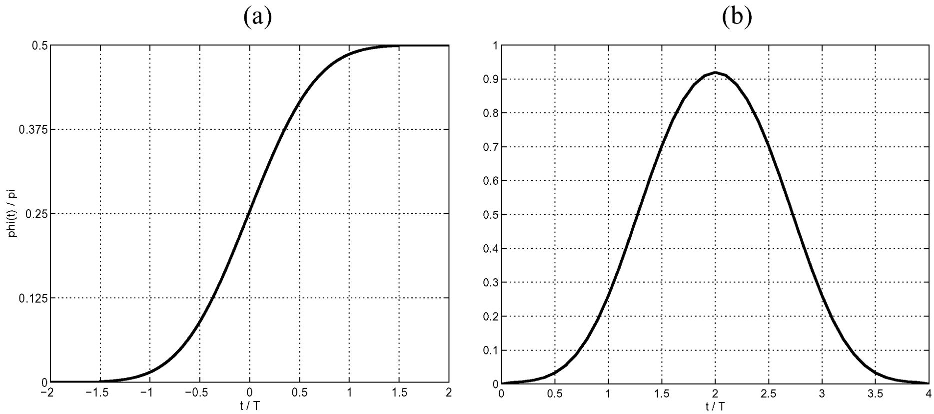

Fig. 1. (a) Phase impulse response $\phi(t)$ of the GMSK modulation, (b) GMSK pulse shape filter $f(t)$.

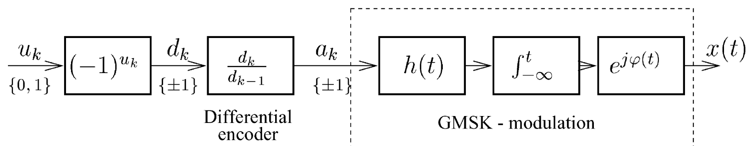

Fig. 2. Signal flow diagram for the GMSK modulation.

is the continuous modulated phase, $\phi(t)$ is the "phase impulse response", $\{a_k\}$ are the differentially encoded symbols from the original data $d_k \in \{-1, 1\}$ and T is the symbol period. The phase impulse response is obtained by integrating a Gaussian filter $h(t) = (1/\sqrt{2\pi}\sigma T)\mathrm{e}^{-(t^2/2\sigma^2 T^2)}$, so $\phi(t) = \pi/2\int_{-\infty}^{t} \mathrm{rect}(u/T)h(u)\,\mathrm{d}u = \pi/2[G(u+\frac{1}{2}) - G(u-\frac{1}{2})]$ where $\sigma = (\sqrt{\ln(2)}/2\pi BT)$, B is the 3 dB bandwith, $BT = 0.3$, and $G(u) = \sigma^2 T\, h(uT) + u\int_{-\infty}^{uT} h(t)\,\mathrm{d}t$. It can be seen in Fig. 1a that $\phi(t)$ can be approximated by zero for $t < -3T/2$ and by $\pi/2$ for $t > 3T/2$. Interpreting this figure, we can conclude that one symbol a_k will have an influence on three symbol periods $(k-1, k, k+1)$.

Considering the data $\{d_k\}$, the differential encoder (see Fig. 2) yields $a_k = d_k d_{k-1} = d_k/(d_{k-1})$. The relation between $\{d_k\}$ and $\{a_k\}$ is such that $a_k = 1$ if $d_k = d_{k-1}$ and $a_k = -1$ if $d_k = -d_{k-1}$. This implies that the phase increases by $\pi/2$ over three symbol periods if the symbols d_k at instants k and $k-1$ are equal and decreases by the same quantity in the other case. We have a modulation with memory in which some ISI gets introduced by the modulation itself.

A sampled GMSK signal can be approximated by a linear filter with impulse response duration of about $L_f T = 4T$ (see Fig. 1b), fed by $b_k = \mathrm{j}^k d_k$ $(\mathrm{j} = \sqrt{-1})$, a modulated version of the transmitted symbols. Such a scheme (but with a shorter filter) holds exactly true when sampled MSK signals are considered [7]. Exploiting the quasi-band-limited character of the GMSK signal, we can even approximate the continuous-time GMSK signal by interpolating the output of a discrete-time linear system. To this end, we shall assume that sampling the GMSK signal at rate r/T satisfies the Nyquist theorem. The linear system $\boldsymbol{F}$ that models the oversampled GMSK signal will be determined by least-squares estimation over a long stretch of signal, see Fig. 3 (alternatively, we could have used the "main" pulse in Laurent's decomposition [7]; however, the linearized model

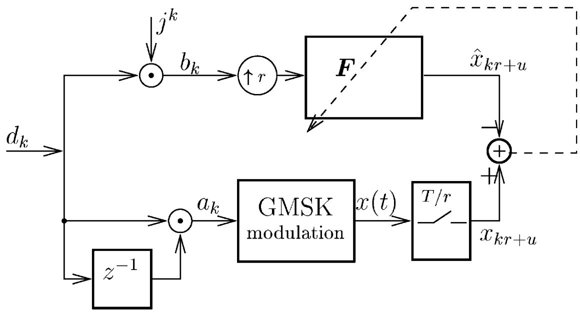

Fig. 3. Identification of the GMSK modulation by least squares.

we obtain is an optimal approximation in the least-squares sense).

Let $\{f_{ir+u}\}_{0\leqslant i\leqslant L_f-1;0\leqslant u\leqslant r-1}$ be the impulse response of the system $\boldsymbol{F}$ thus identified, then

$$x\left(t_0 + kT + u\frac{T}{r}\right) = x_{kr+u} \approx \hat{x}_{kr+u}$$

$$= \sum_{i=0}^{L_f-1} f_{ir+u}\ b_{k-i} \qquad (2)$$

and after interpolation

$$x(t) \approx \hat{x}(t) = \sum_{k=-\infty}^{+\infty} f(t-kT)b_k \qquad (3)$$

where

$$f(t) = \sum_{i=0}^{L_f-1}\sum_{u=0}^{r-1} \operatorname{sinc}\left(r\frac{t-t_0}{T} - ir - u\right) f_{ir+u}$$

(see Fig. 1b).

To have an idea of the quality of this approximation, we plot in Fig. 4 simultaneously the real part of the baseband GMSK signal $x(t)$ and its estimate $\hat{x}(t)$ for $r = 6$. The resulting signal-to-noise (approximation error) ratio turns out to be 25 dB. The power of the linearization errors should be added to the actual noise variance to give the equivalent noise variance in what follows (the power spectrum of the linearization errors turns out to be similar to that of the signal itself though and hence is not flat). Henceforth we shall assume that, with the linearization errors accounted for in the noise term, the linear modulation model is accurate.

3. Multichannel data model

Consider the linearized version of the GMSK modulation transmitted over a linear channel

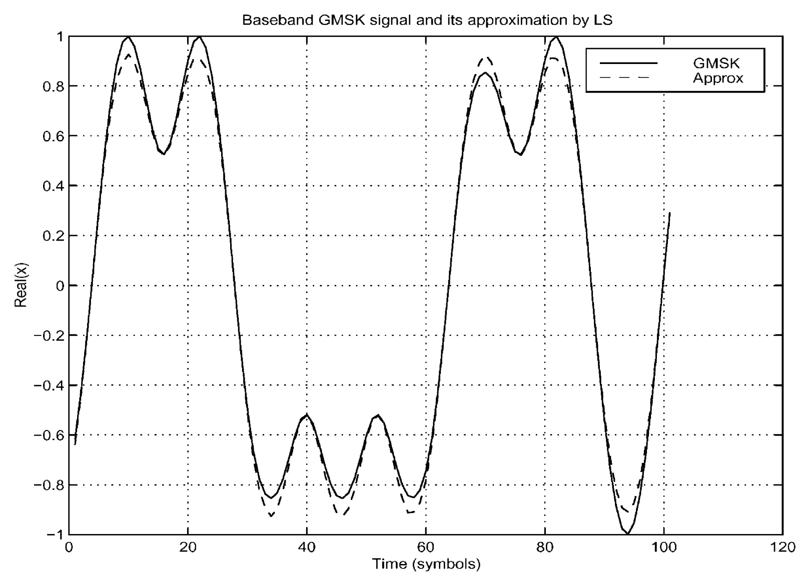

Fig. 4. Linearization of a baseband GMSK signal.

with additive noise. The received signal can be written as

$$y(t) = \sum_k h(t-kT)b_k + v(t)$$

$$= \sum_k h(t-kT)\mathrm{j}^k d_k + v(t), \tag{4}$$

where $h(t)$ is the combined impulse response of the modulation $f(t)$, the propagation channel $c(t)$ and the receiver filter $g(t)$: $h(t) = f(t)c(t)g(t)$. The overall channel impulse response $h(t)$ is assumed to be FIR with duration NT. If K sensors are used and each sensor waveform is oversampled at the rate p/T, the discrete-time input–output relationship at the symbol rate can be written as

$$\boldsymbol{y}'_k = \sum_{i=0}^{N-1} \boldsymbol{h}'_i b_{k-i} + \boldsymbol{v}'_k = \boldsymbol{H}'_N B_N(k) + \boldsymbol{v}'_k,$$

$$\boldsymbol{y}'_k = \begin{bmatrix} y'_{1,k} \\ \vdots \\ y'_{m,k} \end{bmatrix}, \qquad \boldsymbol{v}'_k = \begin{bmatrix} v'_{1,k} \\ \vdots \\ v'_{m,k} \end{bmatrix}, \qquad \boldsymbol{h}'_k = \begin{bmatrix} h'_{1,k} \\ \vdots \\ h'_{m,k} \end{bmatrix}, \tag{5}$$

$$\boldsymbol{H}'_N = [\boldsymbol{h}'_0 \cdots \boldsymbol{h}'_{N-1}], \qquad B_N(k) = [b_k \cdots b_{k-N+1}]^{\mathrm{T}},$$

where the first subscript i denotes the ith channel, $m = pK$, and superscript T denotes transpose. We have introduced the p phases of the K oversampled sensor signals: $y'_{(n-1)p+l,k} = y_n(t_0 + (k + l/p)T)$, $n = 1, \ldots, K$, $l = 1, \ldots, p$ where $y_n(t)$ is the signal received by sensor n.

The propagation environment is described by a channel impulse response $c(t) = [c_1(t) \cdots c_K(t)]^{\mathrm{T}}$. We consider GSM channel models [2] which are taken as specular multipath channels with L_c paths of the form

$$c_n(t) = \sum_{i=1}^{L_c} a_{i,n}\delta(t - \tau - \tau_i) \tag{6}$$

for the nth sensor. $a_{i,n}$ and τ_i are the (complex) amplitude and the delay of path i. The distribution of the amplitudes and the (deterministic) values of the delays depend on the propagation environment (urban, rural, hilly terrain). For the multi-user environment to be considered below, a user-dependent delay τ has been introduced which is taken as uniformly distributed over one symbol period. We consider the channels to be independent across the K sensors (full diversity). A simple calculation shows that the differential delay between sensors can be neglected.

For sake of simplicity, we consider an ideal receiver filter with a half-band of $p/2T$ and a magnitude of $\sqrt{T}$. The overall transmission pulse-shape filter is the convolution of the transmit and the receive filters

$$p_s(t) = \begin{cases} \sqrt{T} \displaystyle\sum_{i=0}^{L_f-1} \sum_{u=0}^{r-1} \mathrm{sinc}\left(r\frac{t-t_0}{T} - ir - u\right) f_{ir+u} \\ \quad \text{if } p > r, \\ \dfrac{p}{r}\sqrt{T} \displaystyle\sum_{i=0}^{L_f-1} \sum_{u=0}^{r-1} \mathrm{sinc}\left(p\frac{t-t_0}{T} - ip - u\frac{p}{r}\right) f_{ir+u} \\ \quad \text{if } p \leqslant r. \end{cases} \tag{7}$$

Then, the received signal for sensor n can be written as

$$y_n(t) = \sum_{k=-\infty}^{+\infty} h_n(t-kT)b_k + v_n(t),$$

$$h_n(t) = \sum_{i=1}^{L_c} a_{i,n} p_s(t - \tau - \tau_i). \tag{8}$$

The continuous-time channel $h_n(t)$ for the nth sensor when sampled at the instant $t_0 + (k + l/p)T$ yields the $((n-1)p + l)$th component of the vector $\boldsymbol{h}'_k$. Furthermore, the sampled (filtered white) noise (with $\mathcal{N}_0/2$ as the power spectrum density of the real or the imaginary part) at the rate p/T is still white with variance $\sigma_v^2 = p\mathcal{N}_0$. Since the GMSK modulation is band-limited, the diversity obtained by oversampling is limited. In practice, typically $p = 2$. Note that p, which is a design parameter at the receiver, is independent of r, which is typically much larger and is chosen to satisfy the Nyquist criterion.

The constellation for the symbols b_k, which are the input to the discrete-time multichannel, is complex whereas the constellation for the symbols d_k is real. It will be advantageous to express everything in terms of real quantities and in this way double the number of (fictitious) channels. To that end we demodulate the received signal by j^{-k} [6]:

$$\begin{aligned} \mathrm{j}^{-k}\boldsymbol{y}'_k &= \sum_{i=0}^{N-1} \mathrm{j}^{-k}\boldsymbol{h}'_i b_{k-i} + \mathrm{j}^{-k}\boldsymbol{v}'_k \\ &= \sum_{i=0}^{N-1} (\mathrm{j}^{-i}\boldsymbol{h}'_i) d_{k-i} + \mathrm{j}^{-k}\boldsymbol{v}'_k \end{aligned} \tag{9}$$

and then we decompose the complex quantities into their real and imaginary parts like

$$\begin{aligned} \boldsymbol{y}^{\mathrm{R}}_k &= \mathrm{Re}(\mathrm{j}^{-k}\boldsymbol{y}'_k) = \sum_{i=0}^{N-1} \mathrm{Re}(\mathrm{j}^{-i}\boldsymbol{h}'_i) d_{k-i} + \mathrm{Re}(\mathrm{j}^{-k}\boldsymbol{v}'_k) \\ &= \boldsymbol{H}^{\mathrm{R}}(q) d_k + \boldsymbol{v}^{\mathrm{R}}_k, \\ \boldsymbol{y}^{\mathrm{I}}_k &= \mathrm{Im}(\mathrm{j}^{-k}\boldsymbol{y}'_k) = \sum_{i=0}^{N-1} \mathrm{Im}(\mathrm{j}^{-i}\boldsymbol{h}'_i) d_{k-i} + \mathrm{Im}(\mathrm{j}^{-k}\boldsymbol{v}'_k) \\ &= \boldsymbol{H}^{\mathrm{I}}(q) d_k + \boldsymbol{v}^{\mathrm{I}}_k, \end{aligned} \tag{10}$$

where q^{-1} is the delay operator: $q^{-1}\boldsymbol{y}_k = \boldsymbol{y}_{k-1}$ and $\boldsymbol{H}^{\mathrm{R}}(q) = \sum_{i=0}^{N-1}\boldsymbol{h}^{\mathrm{R}}_i q^{-i} = \sum_{i=0}^{N-1}\mathrm{Re}(\mathrm{j}^{-i}\boldsymbol{h}'_i)q^{-i}$ and similarly for $\boldsymbol{H}^{\mathrm{I}}(q)$. We can represent this system, with one input and $2m = 2pK$ outputs, more conveniently in the following obvious notation:

$$\boldsymbol{y}_k = \begin{bmatrix} \boldsymbol{y}^{\mathrm{R}}_k \\ \boldsymbol{y}^{\mathrm{I}}_K \end{bmatrix} = \begin{bmatrix} \boldsymbol{H}^{\mathrm{R}}(q) \\ \boldsymbol{H}^{\mathrm{I}}(q) \end{bmatrix} d_k + \begin{bmatrix} \boldsymbol{v}^{\mathrm{R}}_k \\ \boldsymbol{v}^{\mathrm{I}}_k \end{bmatrix} = \boldsymbol{H}(q) d_k + \boldsymbol{v}_k. \tag{11}$$

4. Matched filter bound

The MFB as considered here is a SNR-like quantity. The MFB bounds the probability of error (P_{e}) in the sense that the P_{e} (of e.g. MLSE) is lower bounded by the P_{e} of an additive white Gaussian noise (AWGN) channel with the MFB as SNR (signal-to-noise ratio). MFBs for the multichannel case are discussed in [10] while they are analyzed in [12] in the presence of interferers. The MFB can be obtained by considering the MLSE detection problem of one symbol of the user of interest, assuming perfect knowledge of all past and future symbols. The MFB expressions below will be derived in the case of burst (packet) transmission where the channel for the user of interest can be considered as constant during the transmission of a burst. Since in that case the MFB is symbol-dependent [10], we will consider the average MFB over the burst. Assume we receive M samples:

$$\boldsymbol{Y} = \mathscr{T}(\boldsymbol{H})D + \boldsymbol{V}, \tag{12}$$

where $\boldsymbol{Y} = [\boldsymbol{y}_M^{\mathrm{T}} \cdots \boldsymbol{y}_1^{\mathrm{T}}]^{\mathrm{T}}$ and similarly for $\boldsymbol{V}$ and D, and $\mathscr{T}(\boldsymbol{H})$ is a block Toeplitz matrix with M block rows and $[\boldsymbol{h}_0 \cdots \boldsymbol{h}_{N-1}\ 0_{2m\times(M-1)}]$ as first block row. Let $R_{vv} = \mathrm{E}\boldsymbol{V}\boldsymbol{V}^{\mathrm{H}}$ where the superscript H denotes Hermitian transpose. We shall consider the MFB for MLSE in which the noise covariance matrix is assumed to be $\hat{R}_{vv}$ whereas its actual value is R_{vv}. MLSE boils down to the following weighted least-squares (WLS) problem:

$$\min_{d_k\in\mathscr{C}} \|\boldsymbol{Y} - \mathscr{T}D\|^2_{\hat{R}^{-1}_{vv}}, \tag{13}$$

where $\mathscr{C}$ ($=\{+1, -1\}$ in our case) is the symbol constellation alphabet. So we shall concentrate on the detection of one symbol d_k, the other symbols in D are assumed to be known (detected correctly). For that purpose, we decompose as in [11] the quantity $\mathscr{T}D$ as follows:

$$\mathscr{T}D = \mathscr{T}_{\bar{\mathrm{D}}_k}\bar{\mathrm{D}}_k + \mathscr{T}_{d_k} d_k, \tag{14}$$

$\mathscr{T}_{d_k}$ is the column of $\mathscr{T}$ that gets multiplied by d_k in D, $\mathscr{T}_{\bar{\mathrm{D}}_k}$ is the matrix $\mathscr{T}$ from which the column $\mathscr{T}_{d_k}$ has been eliminated, $\bar{\mathrm{D}}_k$ contains past and future symbols w.r.t. d_k. $\mathscr{T}_{d_k} d_k$ contains the contribution in $\mathscr{T}D$ from the symbol d_k to be detected, and $\mathscr{T}_{\bar{\mathrm{D}}_k}\bar{\mathrm{D}}_k$ the contribution from the other symbols. Since these symbols are known, we can remove their contribution from the received signal. Then, criterion (13) can be rewritten as

$$\min_{d_k\in\mathscr{C}} \|[\boldsymbol{Y} - \mathscr{T}_{\bar{\mathrm{D}}_k}\bar{\mathrm{D}}_k] - \mathscr{T}_{d_k} d_k\|^2_{\hat{R}^{-1}_{vv}}. \tag{15}$$

Its solution gives

$$\begin{aligned} \hat{\mathrm{d}}_k &= \mathrm{dec}\{z_k\}, \\ z_k &= (\mathscr{T}^{\mathrm{H}}_{d_k}\hat{R}^{-1}_{vv}\mathscr{T}_{d_k})^{-1}\mathscr{T}^{\mathrm{H}}_{d_k}\hat{R}^{-1}_{vv}[\boldsymbol{Y} - \mathscr{T}_{\bar{\mathrm{D}}_k}\bar{\mathrm{D}}_k], \end{aligned} \tag{16}$$

where dec{.} is the decision operation that chooses the element in the alphabet $\mathscr{C}$ closest to its argument. $\mathscr{T}^{\mathrm{H}}_{d_k}\hat{R}^{-1}_{vv}$ corresponds to a matched filter, which maximizes the SNR at its output. Further analysis of (16) leads to an interpretation in terms of a non-causal decision feedback equalizer structure [11] for the colored noise case. By definition, the

SNR at the input to the slicer dec{.} is the MFB. For the kth symbol, with $\mathcal{T}_{d_k} = T_k$, we can write

$$\mathrm{MFB}_k = \mathrm{SNR}_k = \frac{\sigma_d^2 (T_k^{\mathrm{H}} \hat{R}_{\upsilon\upsilon}^{-1} T_k)^2}{T_k^{\mathrm{H}} \hat{R}_{\upsilon\upsilon}^{-1} R_{\upsilon\upsilon} \hat{R}_{\upsilon\upsilon}^{-1} T_k}. \tag{17}$$

Due to edge effects, this value depends on the position of the symbols in the burst. We shall consider the average MFB per symbol:

$$\begin{aligned}\mathrm{MFB} &= \frac{1}{M+N-1} \sum_{k=-N+2}^{M} \mathrm{MFB}_k \\ &= \frac{1}{M+N-1} \sum_{k=-N+2}^{M} \frac{\sigma_d^2 (T_k^{\mathrm{H}} \hat{R}_{\upsilon\upsilon}^{-1} T_k)^2}{T_k^{\mathrm{H}} \hat{R}_{\upsilon\upsilon}^{-1} r_{\upsilon\upsilon} \hat{R}_{\upsilon\upsilon}^{-1} T_k}.\end{aligned} \tag{18}$$

Asymptotically in burst length, this formula leads to the equivalent continuous (as opposed to burst-mode) processing MFB. To find the asymptotic expression, we rely on Theorem 4.4 in [5]. Let

$$\mathcal{T}(s_k(z)) = \begin{bmatrix} r_{0,k} & r_{1,k} & \cdots & r_{L,k} \\ r_{-1,k} & \ddots & \ddots & \vdots \\ \vdots & \ddots & \ddots & r_{1,k} \\ r_{-L,k} & \cdots & r_{-1,k} & r_{0,k} \end{bmatrix} \tag{19}$$

be the $(L+1)\times(L+1)$ (block) Toeplitz matrix corresponding to the kth spectrum $s_k(z) = \sum_{i=-\infty}^{\infty} r_{i,k} z^{-i}$. Then, as $L \to \infty$, the following expression

$$\left[\prod_k \mathcal{T}^{\varepsilon_k}(s_k(z))\right]_{i,j} = \frac{1}{2\pi j} \oint \frac{\mathrm{d}z}{z} z^{j-i} \prod_k s_k^{\varepsilon_k}(z) \tag{20}$$

holds for the (i,j)th term of the product of the Toeplitz matrices or their inverse ($\varepsilon_k = \pm 1$). Now, we find for

$$\begin{aligned} T_k^{\mathrm{H}} \hat{R}_{\upsilon\upsilon}^{-1} T_k &= \sum_{i=0}^{N-1} \sum_{j=0}^{N-1} \boldsymbol{h}_i^{\mathrm{H}} [\hat{R}_{\upsilon\upsilon}^{-1}]_{M-k+1-i, M-k+1-j} \boldsymbol{h}_j \\ &\xrightarrow{M\to\infty} \frac{1}{2\pi j} \oint \frac{\mathrm{d}z}{z} \sum_{i=0}^{N-1} \sum_{j=0}^{N-1} \boldsymbol{h}_i^{\mathrm{H}} z^{i-j} \hat{S}_{\upsilon\upsilon}^{-1}(z) \boldsymbol{h}_j \\ &= \frac{1}{2\pi j} \oint \frac{\mathrm{d}z}{z} \boldsymbol{H}^{\dagger}(z) \hat{S}_{\upsilon\upsilon}^{-1}(z) \boldsymbol{H}(z) \end{aligned} \tag{21}$$

and similarly for the denominator. So we get for the continuous processing MFB

$$\mathrm{MFB} = \frac{\sigma_d^2 ((1/2\pi j) \oint (\mathrm{d}z/z) \boldsymbol{H}^{\dagger}(z) \hat{S}_{\upsilon\upsilon}^{-1} \boldsymbol{H}(z))^2}{(1/2\pi j) \oint (\mathrm{d}z/z) \boldsymbol{H}^{\dagger}(z) \hat{S}_{\upsilon\upsilon}^{-1} S_{\upsilon\upsilon} \hat{S}_{\upsilon\upsilon}^{-1} \boldsymbol{H}(z)}, \tag{22}$$

where $S_{\upsilon\upsilon}(z)$ is the power spectral density matrix of υ_k and $\boldsymbol{H}^{\dagger}(z) = \boldsymbol{H}^{\mathrm{H}}(1/z^*)$.

5. Interference cancellation performance bounds

In this section we consider $\hat{S}_{\upsilon\upsilon}(z) = S_{\upsilon\upsilon}(z)$. We define the SNR w.r.t. the additive white noise (the $\sigma_v^2 I_{2m}$ component in $S_{\upsilon\upsilon}(z)$) in the data model (11) as the average SNR per physical channel:

$$\mathrm{SNR} = \frac{1}{2K} \frac{\sigma_d^2}{\sigma_v^2} \frac{1}{2\pi j} \oint \frac{\mathrm{d}z}{z} \boldsymbol{H}^{\dagger}(z) \boldsymbol{H}(z), \tag{23}$$

where σ_v^2 is in fact proportional to the oversampling factor p. We shall consider the additive noise υ_k to consist of d interferers plus spatially and temporally white noise

$$S_{\upsilon\upsilon}(z) = \sigma_d^2 \boldsymbol{G}(z) \boldsymbol{G}^{\dagger}(z) + \sigma_v^2 I_{2m}, \tag{24}$$

where $\boldsymbol{G}(z) = [\boldsymbol{G}_1 \cdots \boldsymbol{G}_d]$ has dimensions $2m \times d$ and $\boldsymbol{G}_k(z)$ has the same structure as $\boldsymbol{H}(z)$. We can define

$$\mathrm{SIR}_k = \frac{\oint (\mathrm{d}z/z) \boldsymbol{H}^{\dagger}(z) \boldsymbol{H}(z)}{\oint (\mathrm{d}z/z) \boldsymbol{G}_k^{\dagger}(z) \boldsymbol{G}_k(z)} \tag{25}$$

as the signal to interference ratio for the kth interferer. With $\hat{S}_{\upsilon\upsilon}(z) = S_{\upsilon\upsilon}(z)$, we get for the MFB from (22)

$$\mathrm{MFB}(\mathrm{SNR}, \mathrm{SIR}) = \frac{\sigma_d^2}{2\pi \mathrm{j}} \oint \frac{\mathrm{d}z}{z} \boldsymbol{H}^{\dagger}(z) S_{\upsilon\upsilon}^{-1} \boldsymbol{H}(z), \tag{26}$$

where we assumed for simplicity that all SIR_k are equal ($=$ SIR). If the multiple users would be detected jointly, a bound on the detection performance for the user of interest is obtained by assuming that the interferers are detected perfectly (in which case their signal contribution can be cancelled perfectly). This leads to $\mathrm{MFB_{JD}} = \mathrm{MFB}(\mathrm{SNR}, \infty) = 2\mathrm{K}\,\mathrm{SNR}$. Here we consider single-user detection, treating the interferers as colored Gaussian noise.

MFB(SNR,SIR) is then the MFB for MLSE in which we take the correlation of the interferers and noise into account properly. By doing so, the multichannel aspect allows for some interference suppression. In order to get a feeling for how much interference suppression is possible, we compare to $\mathrm{MFB_{JD}}$ and introduce

$$\mathrm{MFB_{rel}} = \frac{\mathrm{MFB(SNR,SIR)}}{\mathrm{MFB(SNR,\infty)}} = \frac{\sigma_{\mathrm{v}}^2 \oint (\mathrm{d}z/z)\boldsymbol{H}^{\dagger}(z) S_{vv}^{-1}\boldsymbol{H}(z)}{\oint (\mathrm{d}z/z)\boldsymbol{H}^{\dagger}(z)\boldsymbol{H}(z)}. \tag{27}$$

It can be shown that in general

$$\sin^2\theta = 1 - \frac{\oint (\mathrm{d}z/z)\boldsymbol{H}^{\dagger}(z) P_{\boldsymbol{G}(z)}\boldsymbol{H}(z)}{\oint (\mathrm{d}z/z)\boldsymbol{H}^{\dagger}(z)\boldsymbol{H}(z)} \leqslant \mathrm{MFB_{rel}} \leqslant 1, \tag{28}$$

where $P_{\boldsymbol{G}(z)} = \boldsymbol{G}(z)(\boldsymbol{G}^{\dagger}(z)\boldsymbol{G}(z))^{-1}\boldsymbol{G}^{\dagger}(z)$ is the projection matrix onto the column space of $\boldsymbol{G}(z)$, and θ is the angle between the (subspace spanned by the) interferers and the user of interest. The upper bound is attained as $\mathrm{SIR/SNR} \to \infty$ (even if $\hat{S}_{vv} \neq S_{vv}$, as long as $\hat{S}_{vv}$ also converges to a multiple of the identity matrix) whereas the lower bound is attained as $\mathrm{SIR/SNR} \to 0$. In this latter case, we can only cancel the part of the interferers which is orthogonal to the user of interest. Nevertheless, this shows that when the user of interest is roughly orthogonal to the strong interferers, something that is more likely to happen when more channels are available, then multichannel MLSE which takes the correlation of the noise and interferers into account leads to limited performance loss compared to joint detection, regardless of the strength of the interferers.

6. Optimal spatial filtering

Consider now the problem of optimally combining the phases of the received signal by a purely spatial filter. For a real constellation, the classical $1 \times K$ filter $\boldsymbol{W}$ should be replaced by a $1 \times 2K$ widely linear spatial filter $\boldsymbol{W} = [\boldsymbol{w}^{\mathrm{R}}\boldsymbol{w}^{\mathrm{I}}]$ [1,8] to handle the non-circularity aspect. One can design $\boldsymbol{W}$ by maximizing the signal to interference plus noise ratio (SINR) of the resulting scalar output $\boldsymbol{w}^{\mathrm{R}}\boldsymbol{y}^{\mathrm{R}} + \boldsymbol{w}^{\mathrm{I}}\boldsymbol{y}^{\mathrm{I}}$ where $p = 1$. Then the spatial filter is obtained by maximizing

$$\mathrm{SINR} = \sigma_d^2 \frac{\boldsymbol{W}(1/2\pi j \oint (\mathrm{d}z/z)\boldsymbol{H}(z)\boldsymbol{H}^{\dagger}(z))\boldsymbol{W}^{\mathrm{H}}}{\boldsymbol{W} r_{vv}(0)\boldsymbol{W}^{\mathrm{H}}} = \frac{\boldsymbol{W} r_{yy}(0)\boldsymbol{W}^{\mathrm{H}}}{\boldsymbol{W} r_{vv}(0)\boldsymbol{W}^{\mathrm{H}}} - 1, \tag{29}$$

yielding the generalized eigenvector that is associated to the maximum generalized eigenvalue of the matrices $(r_{yy}(0), r_{vv}(0))$. It follows that

$$\mathrm{SINR} = \lambda_{\max}(r_{vv}^{-1}(0) r_{yy}(0)) - 1 = \sigma_d^2 \lambda_{\max}(r_{vv}^{-1}(0)\boldsymbol{H}_N\boldsymbol{H}_N^{\dagger}). \tag{30}$$

In the case $\mathrm{SIR} \to \infty$, or if the channel of the user of interest is orthogonal to that of the interferers, we have the following equality and bounds for the SINR of optimal spatial filtering in (31) [10]:

$$1 \leqslant \frac{\mathrm{MFB_{JD}}}{\mathrm{SINR}} = \frac{\mathrm{tr}(\boldsymbol{H}_N\boldsymbol{H}_N^{\mathrm{H}})}{\lambda_{\max}(\boldsymbol{H}_N\boldsymbol{H}_N^{\mathrm{H}})} \leqslant \min(2K, N), \tag{31}$$

where the $\mathrm{MFB_{JD}}$ is the MFB for the case of joint detection (or absence of interferers). The lower bound can be reached when the spatio-temporal channel factors into a spatial filter $\boldsymbol{h}_0$ and a scalar temporal filter $c(z) = \sum_{i=0}^{N-1} c_i z^{-i}$; that is $\boldsymbol{H}(z) = \boldsymbol{h}_0(c(z)/c_0)$ (no spatio-temporal diversity). The upper bound is attained when either $\boldsymbol{H}_N\boldsymbol{H}_N^{\mathrm{H}} \sim I_{2K}$ or $\boldsymbol{H}_N\boldsymbol{H}_N^{\mathrm{H}} \sim I_N$, whichever is of full rank (full spatio-temporal diversity). In that case, the individual channel impulse responses are orthonormal. In a statistical set-up, if the $2K$ channel impulse responses are i.i.d., then the upper bound is approached as the number of sensors grows.

7. Simulations

We consider four typical GSM propagation environments: rural area (RU), hilly terrain (HI), typical urban (TU) and bad urban (BU). For each environment, we consider the 6-tap ($L_c = 6$) statistical channel impulse responses as specified in the ETSI standard [4] and this for both the user of interest and the interferers. The channels for multiple antennas are taken independently. A random delay, taken uniformly over one symbol period, is introduced in the (multi-)channel for each user. We show MFB curves as a function of SIR for a fixed SNR = 20 dB. A different value for the SNR will only lead to a translation of the curves along the diagonal of the first quadrant. However, a value greater than 25 dB (which is the approximation error level of the GMSK linearization) would not make sense. The MFB curves are averaged over 50 realizations of the channel impulse responses, according to one of the four statistical channel models. Apart from the performance of MLSE with optimal handling of the spatio-temporal correlations, we also consider the performance of suboptimal MLSE receivers that only take "spatial" correlation into account and neglect the temporal correlation of the interferers or that go as far as treating the interference plus noise as temporally and spatially white circular noise ($\hat{R}_{vv}$ is a multiple of identity, the multiple being the average value of the diagonal elements of R_{vv}). We also show the SINR curve corresponds to the performance of a purely spatial receiver. We show in solid line the MFB when $\hat{R}_{vv} = R_{vv}$ and, respectively, in dashline and dashdot the case where $\hat{R}_{vv}$ is diagonal (MFBW) or block-diagonal (MFBD). The MFB corresponding to the purely spatial approach is shown by a star (MFBS), and the SINR is shown by a square. We consider in our simulations one or multiple interferers and two combinations of multiple sensors and oversampling. (See Figs. 5–9.)

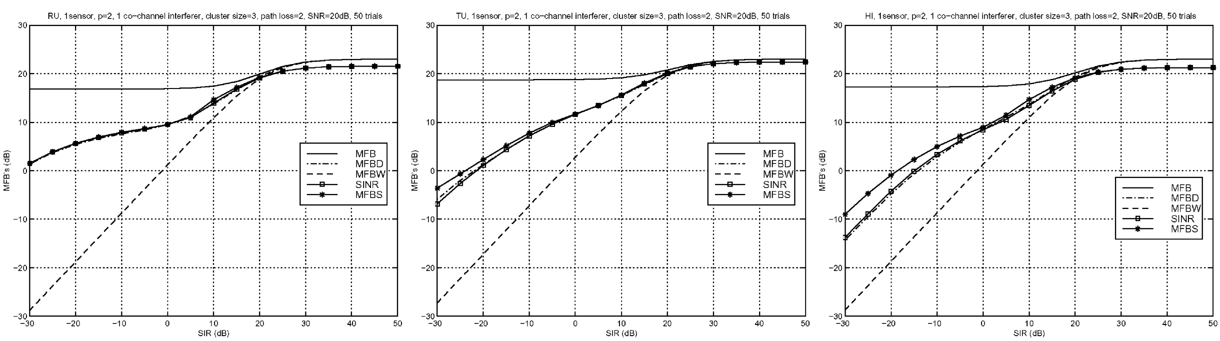

Fig. 5. MFB vs. SIR for SNR = 20 dB, one sensor, one interferer and twofold oversampling, for RU, TU and HI channel models.

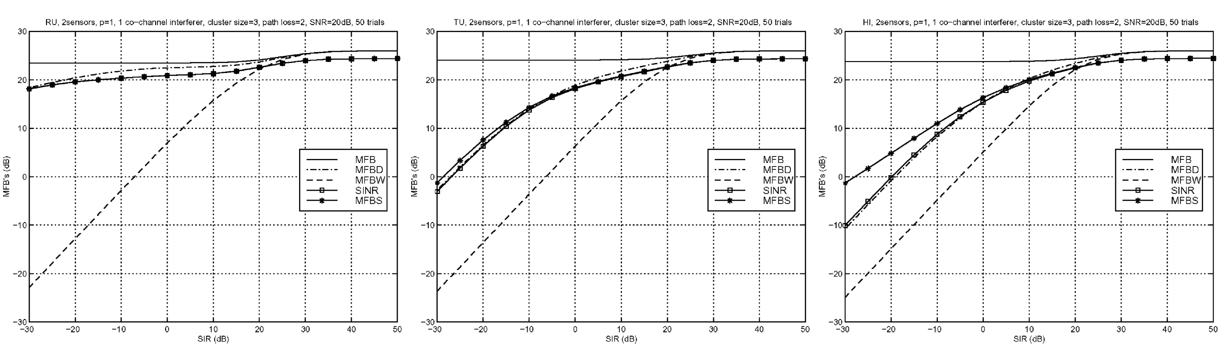

Fig. 6. MFB vs. SIR for SNR = 20 dB, two sensors, one interferer and no oversampling, for RU, TU and HI channel models.

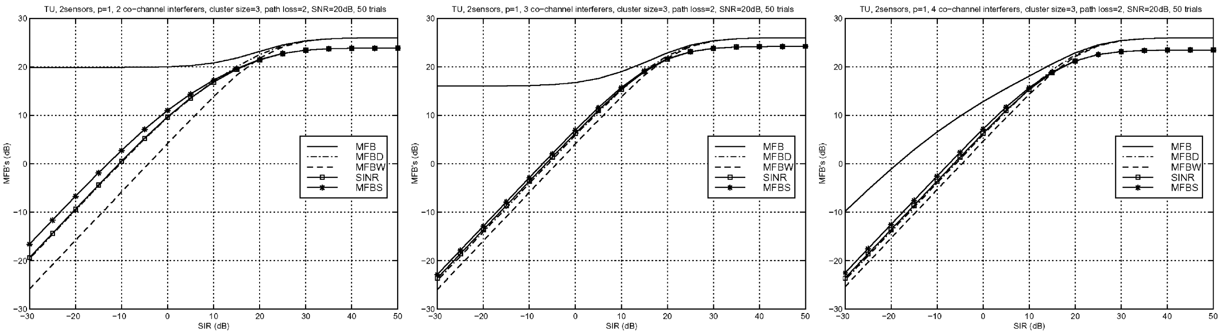

Fig. 7. MFB vs. SIR for SNR = 20 dB, two sensors, no oversampling, the TU channel model, for two, three and four interferers.

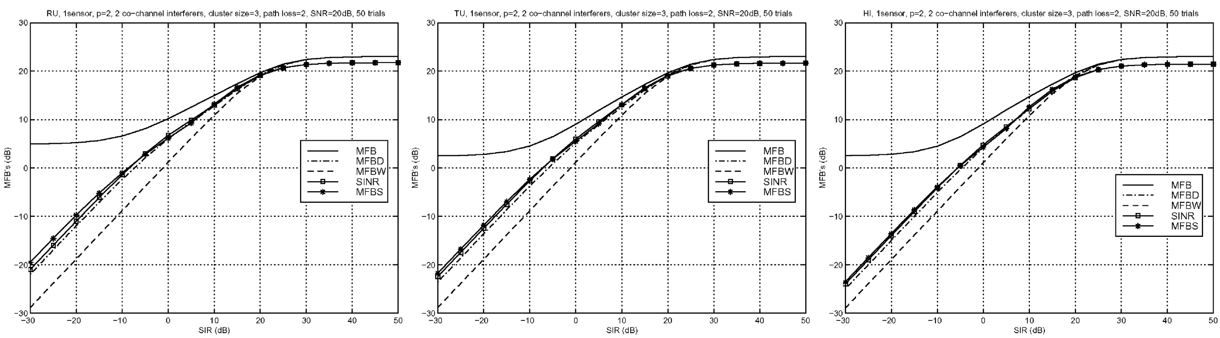

Fig. 8. MFB vs. SIR for SNR = 20 dB, one sensor, two interferers and twofold oversampling, for RU, TU and HI channel models.

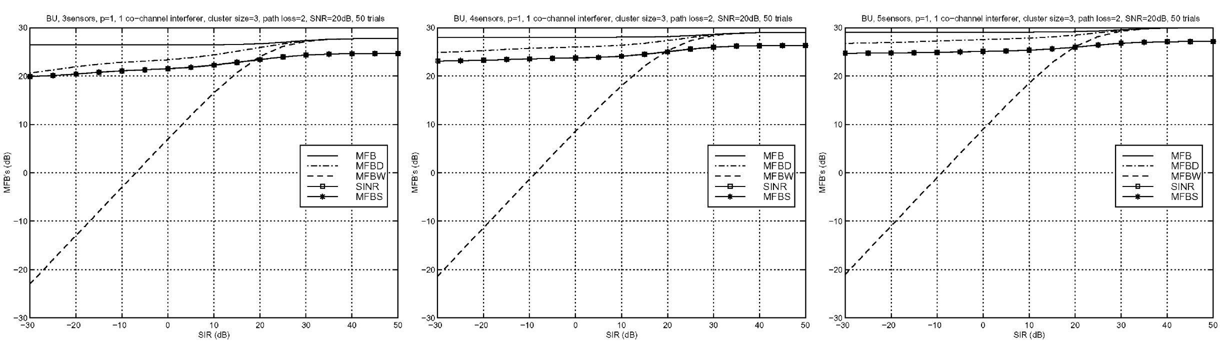

Fig. 9. MFB vs. SIR for SNR = 20 dB, one interferer, no oversampling, for a BU channel model with 3, 4 and 5 sensors.

8. Conclusions

The simulations show that whenever the number of channels is equal or larger than the number of users, then the suboptimal single-user detector which takes the (spatio-temporal) correlation structure of the interferers correctly into account suffers a bounded MFB loss (as the interferers get arbitrarily strong) w.r.t. to the more complex joint detection scheme; there is a floor in the MFB loss. The simulations show that the exploitation of the in-phase and in-quadrature components allows to double the number of channels, with full diversity. Multiple channels obtained by oversampling also lead to bounded loss, be it much larger though. Due to the band-limited nature of GMSK signals, the diversity obtained by oversampling is limited. The simulations show also that, in the case of one interferer, one antenna and twofold oversampling, on the average the loss is bounded by 5 dB. This interference reduction capacity is due almost exclusively to the two-channel aspect created by exploiting the real aspect of the symbol constellation after an appropriate reformulation of GMSK. This loss can be reduced to 2 dB by using two sensors (with complete spatial diversity). The results also show that not taking the noise correlation into account properly (esp. $\hat{R}_{vv} \sim I$, as is done in current GSM receivers) leads to the absence of robustness to interference, while taking only spatial correlation into account ($\hat{R}_{vv}$ block diagonal with $2K \times 2K$ blocks) leads to very limited robustness. The purely spatial approach performs well when the number of sensors is high (greater than three but with the exploitation of the I and the Q parts of the constellation). This result is expected since the channels of the user of interest and the interferers tend to be orthogonal and then the loss in performance is shown to be bounded. It should be noted that the losses shown here are averaged over all possible interferer configurations. The actual loss can be quite a bit less most of the time.

References

[1] P. Chevalier, Filtrage d'Antenne Optimal pour Signaux non Stationnaires. Concepts, Performances, Proceedings of Quinzième Colloque sur le traitement du signal et des images, Juan-les-pins, France, Du 18 au 21 September 1995.

[2] COST 207, Digital land mobile radio communications, Technical Report, Office for Official Publications of the European Communities, Luxembourg, Final Report, 1989.

[3] ETSI Tdoc SMG2 WPB 108/98, EDGE Evaluation of 8-PSK, Technical Report, ETSI, 20–24 April 1998. Kuusamo, Finland.

[4] European Telecommunications Standards Institute, European digital cellular telecommunications system (phase 2): Radio transmission and reception (GSM 05.05), Technical Report, ETSI, December 1995. Sophia Antipolis, France.

[5] R.M. Gray, Toeplitz and circulant matrices: a review, Technical Report, Stanford University, June 1971. Revised April 1977, April 1993. Stanford, California 94305.

[6] M. Kristensson, B.E. Ottersten, D.T.M. Slock, Blind subspace identification of a BPSK communication channel, Proceedings of 30th Asilomar Conference on Signals, Systems and Computers, Pacific Grove, CA, 1996.

[7] P.A. Laurent, Exact and approximate construction of digital phase modulations by superposition of amplitude modulated pulses (AMP), IEEE Trans. Commun. 34 (February 1986).

[8] B. Picinbono, P. Chevalier, Widely linear estimation with complex data, IEEE Trans. Signal Process. 43 (August 1995).

[9] D.T.M. Slock, Blind joint equalization of multiple synchronous mobile users using oversampling and/or multiple antennas, Proceedings of 28th Asilomar Conference on Signals, Systems and Computers, Pacific Grove, CA, October 31–November 2 1994.

[10] D.T.M. Slock, E. De Carvalho, Matched filter bounds for reduced-order multichannel models, Proceedings of Communication Theory Mini-Conference, Globecom, London, England, November 1996.

[11] D.T.M. Slock, E. De Carvalho, Burst mode non-causal decision-feedback equalization and blind MLSE, Proceedings of Communication Theory Mini-Conference, Globecom, London, England, November 1996.

[12] D.T.M. Slock, H. Trigui, An interference cancelling multichannel matched filter, Proceedings of Communication Theory Mini-Conference (Globecom), London, England, November 1996.

[13] B.D. Van Veen, K.M. Buckly, Beamforming: a versatile approach to spatial filtering, IEEE Accoust. Speech Signal Process. Mag. (April 1988).

[14] S. Verdú, Minimum probability of error for asynchronous Gaussian multiple access channels, IEEE Trans. Inform. Theory IT-32 (January 1986) 85–96.

[15] G. Xu, H. Liu, W.J. Vogel, H.P. Lin, S.S. Jeng, G.W. Torrence, Experimental studies of space-division-multiple-access schemes for spectral efficient wireless communications, Proceedings of ICC, New Orleans, LA, USA, 1–5 May 1994.